

Mixed convection heat transfer in trapezoidal lid-driven cavity with uniformly heated inner circular cylinder

ASMAA ALI HUSSEIN*

Middle Technical University, Institute of Technology/Baghdad,
Baghdad, Iraq

Abstract The present work comprises a numerical analysis using the Ansys program to solve the problem of combined free-forced convection around a circular cylinder located in a horizontal lid-driven trapezoidal enclosure. The enclosure is filled with water. The upper moving wall and lower fixed wall are cold at a constant temperature, whereas the inclined walls are adiabatically insulated. The uniformly heated cylinder is located at different positions in the cavity. The study covers three values of Richardson number (0.01, 1, and 10). The results show that the streamlines and isotherms in the enclosure, the Nusselt number and friction factor in the moving wall, hot wall and bottom wall are strongly dependent on the position of the inner hot cylinder. The results are validated with previous work, and the comparison gives good agreement.

Keywords: Cavity; Heat transfer; Mixed convection; Lid-driven

Nomenclature

B_n	–	Bingham number
C_f	–	friction coefficient
Da	–	Darcy number
g	–	gravitational acceleration
Gr	–	Grashof number
H	–	height of cavity
Ha	–	Hartmann number
L	–	side length of cavity
Le	–	Lewis number

*Corresponding Author. Email: asmaa31930@yahoo.com

p	–	pressure
Nu	–	Nusselt number
n	–	coordinate normal to wall
Pr	–	Prandtl number
Re	–	Reynold number
Ri	–	Richardson number
T	–	temperature
T_r	–	freezing point of the base fluid, = 273.15 K
T_0	–	reference temperature, = 310 K
U, V	–	dimensionless velocity in x - and y -direction
u, v	–	velocities in x - and y -direction
u_1	–	velocity of moving wall
x, y	–	Cartesian coordinates

Greek symbols

α	–	thermal diffusivity
β	–	thermal expansion coefficient
γ	–	inclination angle
θ	–	dimensionless temperature
κ	–	thermal conductivity
κ_f, κ_s	–	thermal conductivity for base fluid and nanoparticles
μ	–	dynamic viscosity
ϑ	–	kinematic viscosity
ρ	–	density
φ	–	nanoparticles volume fraction

Subscripts

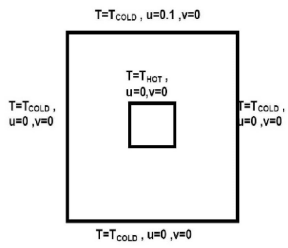
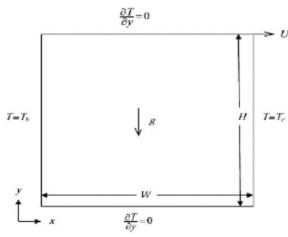
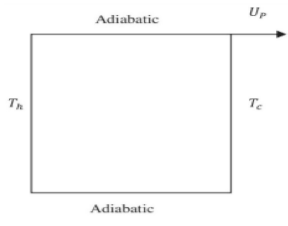
c	–	cold
h	–	hot

1 Introduction

Fluid behaviour and thermal field in lid-driven trapezoidal cavities is a topic of great importance to many researchers due to its significance in practical engineering applications. These applications include solar energy, power stations, heat exchanger devices, nuclear reactors, the technology of lubrication, combustion of atomized liquid fuels and cooling of electronic equipment [1, 2]. The forced convection process is achieved when the fluid motion is caused by using external devices such as a compressor, fan, etc. This process may be occurred by using rotating cylinder in cavity or movement of wall in the cavity (lid-driven cavity). It is characterized by the Reynolds number (Re). The heating of the system causes thermal patterns between the hot wall and the cold fluid and leads to reducing the fluid

density. As a result, the light fluid particles rise upwards while the heavy particles descend downward. The motion of fluid resulting from density changes in the fluid is called free convection. This process is characterized by the Rayleigh number (Ra) or Grashof number (Gr). The Richardson number (Ri) is the ratio between Gr and Re^2 . The value of the Richardson number determines if the process is dominated by forced convection, natural convection, or mixed convection. The mixed convection heat transfer in a lid-driven cavity with different geometries and thermal boundary conditions was studied by many authors [1–24]. The cavity with lid-driven is considered in different shapes, such as square [1–8], trapezoidal (or triangle) [9–13], rectangle [14–18], and other geometries [19–24] with various thermal and hydrodynamic boundary conditions. Tables 1–4 present a summary of these works.

Table 1: Previous works which included square lid-driven cavity.

Geometry	Conditions	Conclusions	Reference
	Air $10^2 \leq Re \leq 10^3$ $Ri = 0.01-10$	Richardson number plays an important role in fashioning of vorticity	Rosdzimin <i>et al.</i> (2010), [1]
	$H_2O-Al_2O_3$, CuO , Cu nanofluids $\varphi = 0-0.05$ $Re = 1, 10, 100$ $Ra = 10^4$	Increasing Re causes reduction of the nanoparticles concentration	Nemati <i>et al.</i> (2010), [2]
	$Water-Al_2O_3$ nanofluid $\varphi = 0-0.06$ $Gr = 10^4$ $Ri = 0.01-100$	The heat transfer enhances as volume fraction of nanoparticles increases	Sheikhzadeh <i>et al.</i> (2012), [3]

Continued on next page

Table 1. Continued from previous page.

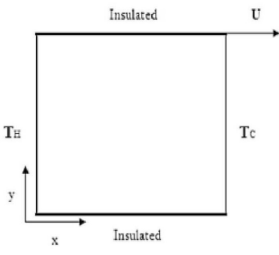
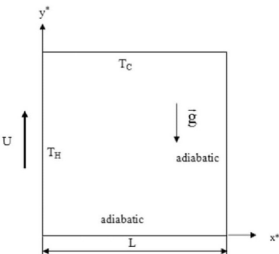
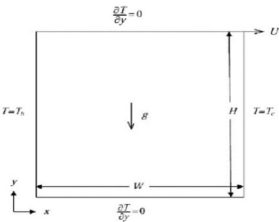
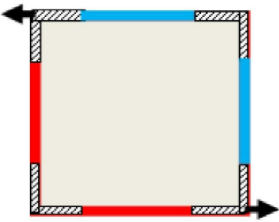
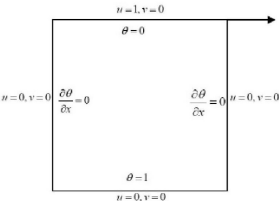
Geometry	Conditions	Conclusions	Reference
	Air $Ri = 1$ $10^{-5} \leq Da \leq 10^{-1}$	The thermal patterns and fluid field depend on the direction of moving walls with nonuniform heating	Chattopadhyay <i>et al.</i> (2014), [4]
	Al_2O_3 + ethylene glycol- H_2O nanofluid $\varphi = 0-0.08$ $Ri = 0.1-10$ $Gr = 10^4$	The thermal patterns and fluid field depend on φ	Öğüt and Kahveci (2016), [5]
	$Cu-H_2O$ nanofluid $\varphi = 0-0.05$ $Ri = 0.01-100$	The maximum heat transfer rate is produced with presence of the shear-driven and the buoyancy forces	Mastiani <i>et al.</i> (2017), [6]
	$Cu-H_2O$ nanofluid $\varphi = 0.05$ $10^3 \leq Gr \leq 10^6$ $1 \leq Re \leq 100$ $10^{-5} \leq Da \leq 10^{-2}$	The heat transfer enhances with decrease in Da	Haque Munshi <i>et al.</i> (2019), [7]
	$Gr = 10^3, 10^5$ $Re = 10-10^3$ $Al_2O_3-H_2O$ nanofluids $\varphi = 0-0.05$	The heat transfer enhances with increase in Re	Çakmak <i>et al.</i> (2020), [8]

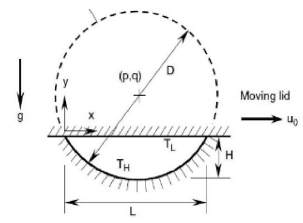
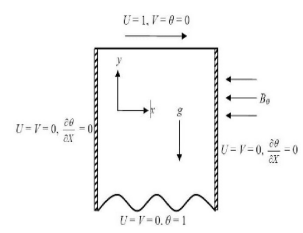
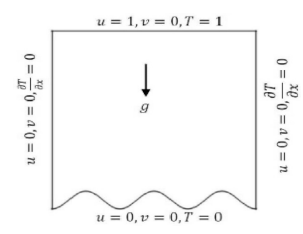
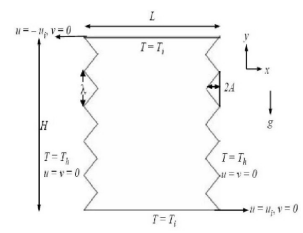
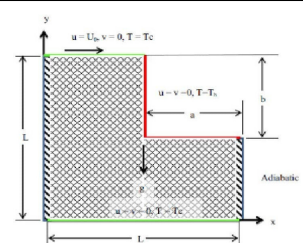
Table 2: Previous works which included trapezoidal lid-driven cavities.

Geometry	Conditions	Conclusions	Reference
<p>T_b (case 1) or $T_c + (T_c - T_b) \sin(2\pi x/L)$ (case 2)</p>	<p>$Pr = 0.015, 0.7, 10$ $Re = 1-100$ $Gr = 10^3 - 10^5$</p>	<p>The bottom wall produces multiple steady states in either natural or mixed convection</p>	<p>Bhattacharya <i>et al.</i> (2013), [9]</p>
	<p>$0.026 \leq Pr \leq 1000$ $10^3 \leq Ra \leq 10^6$ $Ha = 50-1000$</p>	<p>There is no effect of the moving lid for $Ra \geq 10^5$</p>	<p>Mehmod and Tabish (2016), [10]</p>
<p>Case 1</p>	<p>$Le = 0.1-50$ $0.1 \leq Ri \leq 100$</p>	<p>Uniform heat flux concentrated of the fixed horizontal wall has given high mass transfer</p>	<p>Uddin <i>et al.</i> (2016), [11]</p>
<p>$\partial T / \partial y = 0$</p>	<p>$H_2O-Cu, Ag, Al_2O_3, TiO_2$ $0 \leq \varphi \leq 0.02$ $0.04 \leq Ri \leq 100$ $0 \leq Ha \leq 50$</p>	<p>Ha and heat source location produced significant influence on Nusselt number</p>	<p>Ahmed <i>et al.</i> (2018), [12]</p>
<p>Physical Domain</p>	<p>$Pr = 0.7, 1000$ $10^3 \leq Ra \leq 10^5$ $\gamma = 45^\circ - 90^\circ$</p>	<p>The results produced minimum entropy and maximum efficiency of any system</p>	<p>Monda and Mahapatra (2020), [13]</p>

Table 3: Previous works which included rectangular lid-driven cavity.

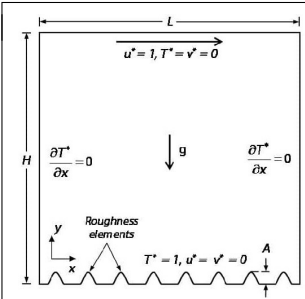
Geometry	Conditions	Conclusions	Reference
	<p>Water $Ra = 10^5 - 10^7$ $Re = 408.21$ $\gamma = 0^\circ - 30^\circ$</p>	<p>The heating process increases as the tilt angle is moved from vertical to horizontal situation</p>	<p>Sharif (2007), [14]</p>
	<p>$0.1 \leq Ri \leq 10$ $0.1 \leq h/H \leq 0.5$ $0.01 \leq \kappa_f/\kappa_s \leq 10$</p>	<p>Nu decrease with increasing the wall thickness ratio</p>	<p>Oztop <i>et al.</i> (2008), [15]</p>
	<p>H₂O-Cu $\gamma = 0^\circ - 30^\circ$ $Ri = 0.1 - 10$ $\varphi = 0.05 - 0.08$</p>	<p>Nu increases strongly as tilt angle is increased for $Ri = 10$</p>	<p>Salahi <i>et al.</i> (2015), [16]</p>
	<p>$Pr = 1$ $Re = 100 - 1000$ $Gr = 10^4$ $Ha = 0 - 5$ $Bn = 1 - 10$</p>	<p>Nu increases with increasing Ha, and with decreasing Bn</p>	<p>Kefayati and Tang (2018), [17]</p>
	<p>Cu-H₂O nanofluid $Gr = 10^4$ $Ri = 0.1 - 10$</p>	<p>The heat transfer increases using Al₂O₃-H₂O nanofluid with increase in for a constant Darcy number</p>	<p>Ardalan <i>et al.</i> (2021), [18]</p>

Table 4: Previous works which included other geometries of lid-driven cavities.

Geometry	Conditions	Conclusions	Reference
	$Pr = 0.71$ (air) $Gr = 0-10^6$ $Re = 0-500$	The influence of inertia force is pronounced for $Gr \leq 10^5$	Chin-Lung and Chin-Hsiang (2004), [19]
	$Pr = 0.71$ $Re = 300$ $Ra = 10^5$ $0 \leq Ha \leq 50$	The average Nu increases with increase in the number of waves and decrease in Ha	Parvin and Nasrin (2010), [20]
	$Pr = 0.71$ $Re = 10^2-5 \cdot 10^3$ $Gr = 10^3-10^6$	The parameters (Re and Gr) affect significantly on the fluid field and thermal patterns	Kumar <i>et al.</i> (2013), [21]
	CuO-H ₂ O nanofluid $Pr = 10, 1.47$ $Ri = 0.1, 1, 10$ $\varphi = 0.04-0.2$	Ri and volume fraction have significant effects on the behavior of heat transfer and fluid flow inside the triangular cavity	Nasrin <i>et al.</i> (2014), [22]
	$Pr = 0.71$ porous media $Re = 1-100$ $Gr = 10^3-10^5$ $Da = 10^{-5}-10^{-3}$	The heat transfer rate in the vertical wall is higher than that in the horizontal wall at a low Gr, higher Da and higher Re	Mojumder <i>et al.</i> (2016), [23]

Continued on next page

Table 4. *Continued from previous page.*

Geometry	Conditions	Conclusions	Reference
	$Pr = 0.7$ $0.01 \leq \varphi \leq 0.08$ $Ra = 10^3 - 10^5$ $Re = 10, 2000$	Significant effects of number and amplitude of roughness elements on the thermal and fluid patterns	Guo <i>et al.</i> (2016), [24]

The motivation of the present simulation is to enhance the heat transfer process inside the trapezoidal cavity because of its importance in mechanical engineering applications. To obtain this goal, the influence of different parameters that affect the heat transfer process should be studied. One of these important parameters is the position of an inner hot cylinder inside the trapezoidal lid-driven cavity for the same condition. Additionally, the influence of the Richardson number on the thermal pattern and fluid velocity requires further study. The working fluid is water. The parallel walls are cooled and the inclined walls are adiabatically insulated. The upper wall only moves as lid-driven at a constant speed, while the other three walls are stationary. The novelty of this work is studying the mixed convection heat transfer inside the cavity at different hot source positions. This work requires advanced computers and more patience with the run time of the program. The simulation was achieved using the Ansys commercial program (ANSYS Fluent 2021 R2).

2 Theoretical analysis

The physical domain for a trapezoidal enclosure with the movement of the top wall at velocity U is shown in Fig. 1. The heating source consists of a circular cylinder located at different positions inside the cavity. The circular hot cylinder is kept constant and the inclined walls are adiabatically insulated. The working fluid is water with $Pr = 6.2$. The combined effect of buoyancy forces due to the temperature difference throughout the fluid and the forced convection effect due to the motion of the top wall of a trapezoidal

cavity is numerically modelled. Table 5 represents the hydrodynamic and thermal boundary conditions for the problem.

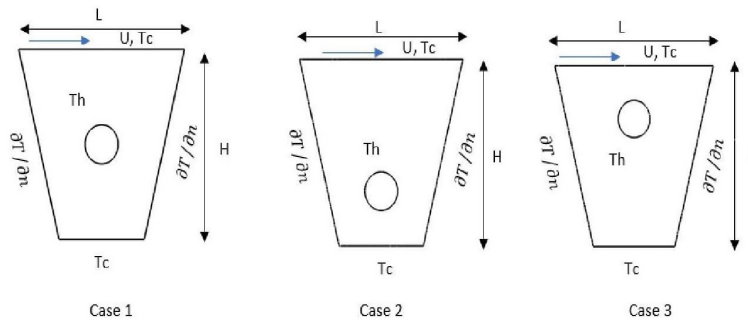


Figure 1: Schematic of physical domain.

Table 5: Boundary conditions for the present study.

Position of wall	U	V	θ
Bottom wall	0	0	0
Top wall	1	0	0
Left and right walls	0	0	$\partial\theta/\partial X = 0$
Circular cylinder wall	0	0	1

2.1 Governing equations

The two-dimensional laminar mixed convection heat transfer in the lid-driven trapezoidal cavity containing concentric and eccentric circular cylinders is represented by governing equations. The water properties are assumed constant except for the density which varies in the buoyancy term according to the Boussinesq approximation. The governing equations include continuity, momentum in x - and y -direction, and energy equations [14]:

$$\frac{\partial u}{\partial x} + \frac{\partial v}{\partial y} = 0, \quad (1)$$

$$u \frac{\partial u}{\partial x} + v \frac{\partial u}{\partial y} = -\frac{1}{\rho} \frac{\partial p}{\partial x} + \nu \left(\frac{\partial^2 u}{\partial x^2} + \frac{\partial^2 u}{\partial y^2} \right), \quad (2)$$

$$u \frac{\partial v}{\partial x} + v \frac{\partial v}{\partial y} = -\frac{1}{\rho} \frac{\partial p}{\partial y} + \nu \left(\frac{\partial^2 v}{\partial x^2} + \frac{\partial^2 v}{\partial y^2} \right) + g\beta(T - T_c), \quad (3)$$

$$u \frac{\partial T}{\partial x} + v \frac{\partial T}{\partial y} = \alpha \left(\frac{\partial^2 T}{\partial x^2} + \frac{\partial^2 T}{\partial y^2} \right). \quad (4)$$

These equations can be normalized by defining the dimensionless variables as follows:

$$X = \frac{x}{L}, \quad Y = \frac{y}{L}, \quad U = \frac{u}{u_1}, \quad V = \frac{v}{u_1}, \quad \theta = \frac{T - T_c}{T_h - T_c}, \quad \text{Re} = \frac{u_1 H}{\vartheta},$$

$$\text{Gr} = \frac{g\beta(T_h - T_c)H^3}{\vartheta^2}, \quad P = \frac{pL^2}{\rho\alpha^2}, \quad \text{Pr} = \frac{\vartheta}{\alpha}, \quad \text{Ri} = \frac{\text{Gr}}{\text{Re}^2}.$$

So, Eqs. (1)–(4) can be written in dimensionless form as shown below:

$$\frac{\partial U}{\partial X} + \frac{\partial V}{\partial Y} = 0, \quad (5)$$

$$U \frac{\partial U}{\partial X} + V \frac{\partial U}{\partial Y} = -\frac{\partial P}{\partial X} + \frac{1}{\text{Re}} \left(\frac{\partial^2 U}{\partial X^2} + \frac{\partial^2 U}{\partial Y^2} \right), \quad (6)$$

$$U \frac{\partial V}{\partial X} + V \frac{\partial V}{\partial Y} = -\frac{\partial P}{\partial Y} + \frac{1}{\text{Re}} \left(\frac{\partial^2 V}{\partial X^2} + \frac{\partial^2 V}{\partial Y^2} \right) + \text{Ri} \theta, \quad (7)$$

$$U \frac{\partial \theta}{\partial X} + V \frac{\partial \theta}{\partial Y} = \frac{1}{\text{Pr Re}} \left(\frac{\partial^2 \theta}{\partial X^2} + \frac{\partial^2 \theta}{\partial Y^2} \right). \quad (8)$$

2.2 Nusselt number and pressure drop losses

The Nusselt number expresses the average heat transfer rate in the system. In the present work, the mean Nusselt number on the moving wall is as follows [14]:

$$\text{Nu} = \int_0^L \text{Nu}_x dx, \quad (9)$$

where Nu_x is the local Nusselt number. Equation (9) can be written as follows:

$$\text{Nu} = \frac{1}{L} \int_0^L \frac{\partial \theta}{\partial X} \Big|_{X=0} dY, \quad (10)$$

where L is the length of wall.

2.3 Validation

The code which is used to obtain the present results is validated by taking a case study investigated by Alesbe *et al.* [25]. The results of streamlines and isotherms for both studies with three values of Richardson numbers are given in Fig. 2. Alesbe *et al.* [25] in their work used a hybrid nanofluid

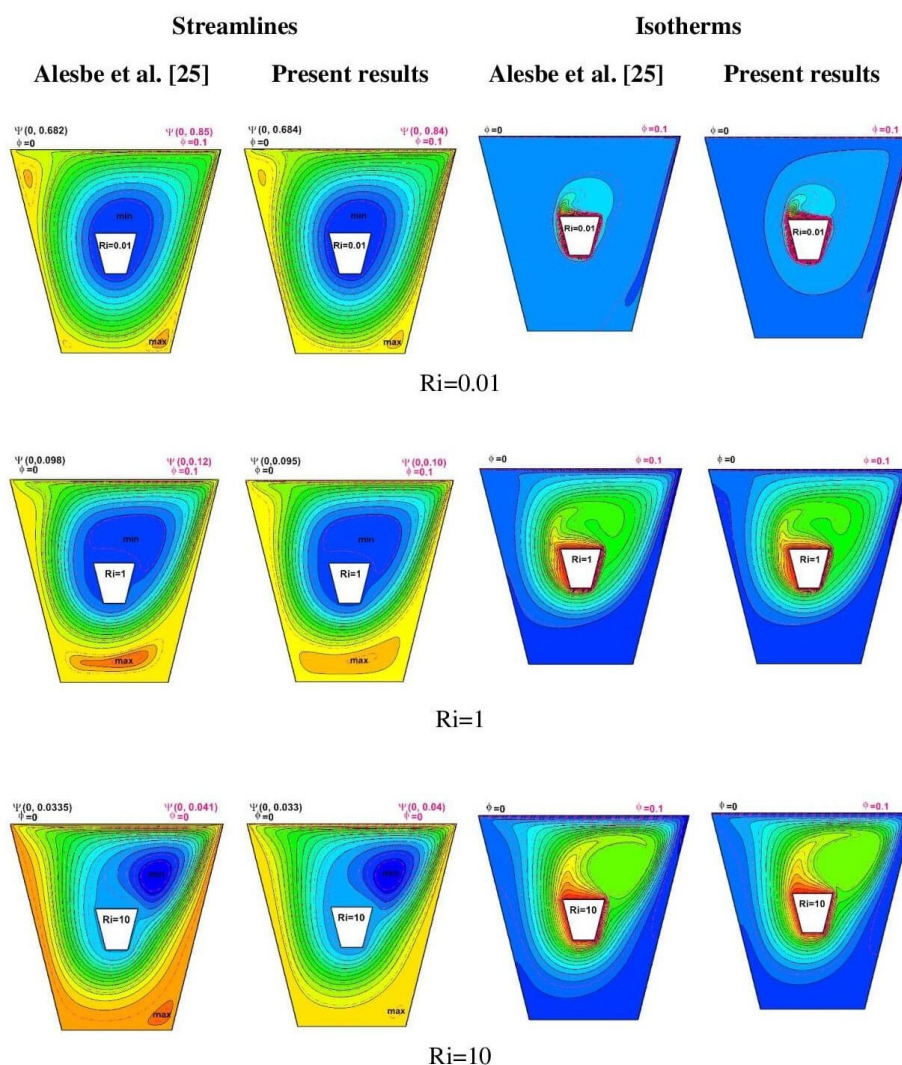


Figure 2: Code validation for the present study (Φ – nanoparticles volume fraction, Ψ – stream function).

in a trapezoidal lid-driven annulus. The comparison has been carried out by moving only the top wall. It is noticed that the comparison gives a good validation for both studies.

3 Numerical results

3.1 Flow field and thermal patterns

The effects of the inner cylinder position as in case 1: concentric annulus; case 2: lower position; case 3: upper position on the behaviour of fluid motion and thermal fields for three Richardson numbers ($Ri = 0.01, 1, \text{ and } 10$) are shown in Figs. 3 and 4, respectively. Generally, the thermal distribution

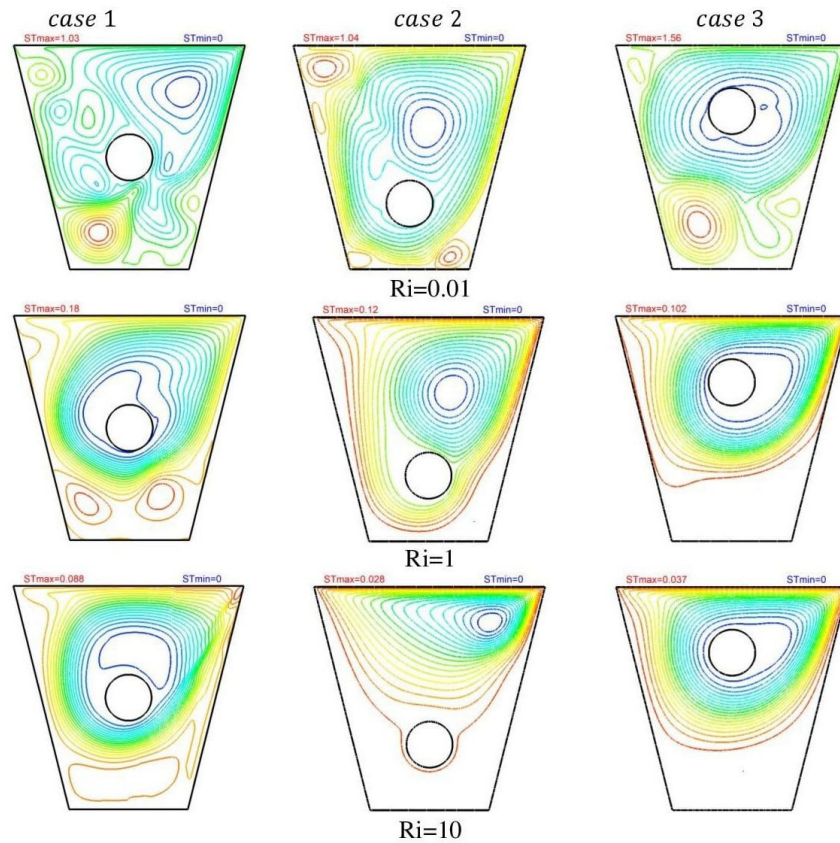


Figure 3: Streamlines in trapezoidal lid driven annulus with different Richardson numbers $Ri = 0.01, 1, \text{ and } 10$ (ST_{\min}, ST_{\max} – minimum and maximum stream function).

inside the enclosure depends greatly on the forced convection flow resulting from moving the top wall. So, at a low Richardson number ($Ri = 0.01$), the shear effects resulting from the motion of the top lid are predominant. This motion of the top wall causes a significant recirculating eddy which will be generated in the corners of the cavity for the three investigated cases. The number of these eddies for the concentric annulus (case 1) is higher than that for the eccentric annuli (cases 2 and 3), especially on the left-hand side of the cavity. As can be seen, higher temperature gradients are formed near the hot cylinder wall. The thermal lines (isotherms) rotate about the hot cylinder. The isotherms get away from the hot cylinder. So, the region seems to be colder than nearby areas because of the dominating forced

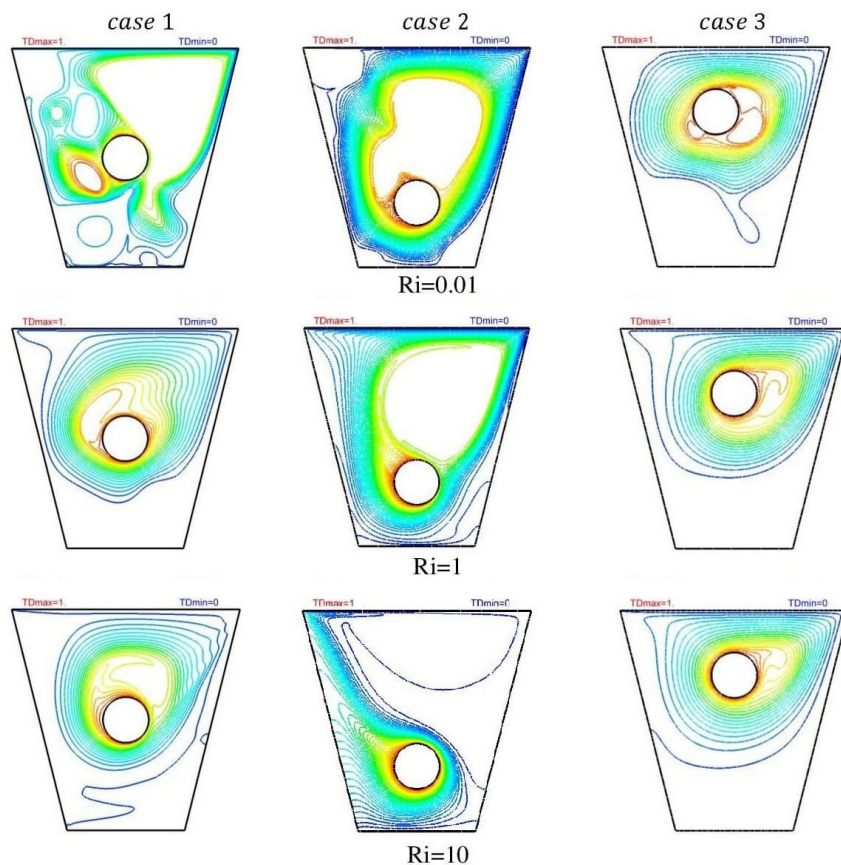


Figure 4: Isotherms in trapezoidal lid driven annulus with different Richardson numbers $Ri = 0.01, 1,$ and 10 (TD_{\min} , TD_{\max} – minimum and maximum temperature difference).

convection. Actually, for forced convection (low Richardson number), the vorticities are stronger at the upper region of the enclosure than those in the mixed and natural convection.

The free convection currents grow as the Richardson number increases and produce circulation. The mini vortices (eddies) diminish in the top region of the annulus at $Ri = 1$ (dominant mixed convection, i.e., the primary and secondary flows are equivalent) for case 1 and case 3 except for case 2 (bottom position of the circular cylinder). Moreover, two eddies will be formed at the lower region of the concentric annulus, while circular lines of fluid velocity will be generated around the hot cylinder in case 3 (top position of the inner cylinder). Moreover, two eddies will be formed at the lower region of the concentric annulus. It is evident that the isotherms move towards the outer cylinder. The higher velocity of the fluid close to the lid-driven wall produces a significant distortion in the thermal plume.

Increasing the buoyancy effects at the expense of inertia force reduces the shear-driven circulation. In this case, the natural convection is dominated ($Ri = 10$). It is noted that the small vortices (eddy) will be eliminated. One large vorticity will be formed. Its centre depends on the position of the inner cylinder. The maximum stream function in case 1 is higher than in case 3 and case 2, consequently. It is expected that the heat transfer rate in case 1 is better than that in case 3 and case 2, respectively. The isotherms in case 1 and case 3 are more uniform than in case 2 because higher natural convection currents in case 2 cause a high temperature gradient, and a large distortion in the thermal plume deviates towards the adiabatic left wall, while the right wall will be cold. Additionally, the bottom region of cases 1 and 3 will be colder than other regions of the cavity; leading to a high heat transfer rate in these cases. Increasing Ri from 1 to 10 leads to the thermal patterns which do not exhibit much change in cases 1 and 3 because the hot cylinder is close to the moving wall in these cases. As a result, the thermal plume will be affected by the motion of fluid near the moving wall.

3.2 Nusselt number

Figure 5 represents the relationship between the mean Nusselt number and Richardson number for three cases studied in the present work, and for three walls for each case: moving wall, bottom wall and hot circular wall. It is shown in this figure that the values of the mean Nusselt number in the moving wall are higher than that in the hot and the bottom walls. This is attributed to the effect of the lid-driven wall to improve the heat transfer

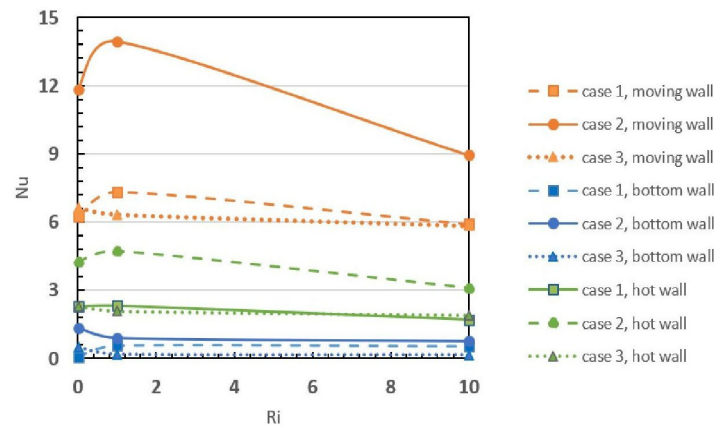


Figure 5: The relation between the mean Nusselt number and the Richardson number for all cases considered.

rate and due to the dominant inertia force in the mechanism of heat transfer. Also, the natural convection currents aid to increase the fluid velocity near the hot wall. This leads to an increase in the rate of heat transfer on the hot wall. Moreover, the maximum value of the Nusselt number in the moving and hot walls for both cases: case 1 (concentric cylinder) and case 2 (lower position of the inner cylinder) occurs at $Ri = 1$ (mixed convection), whereas for case 3 (upper position of the inner cylinder), the maximum Nusselt number occurs at $Ri = 0.01$ (forced convection) in the moving and hot walls. This behaviour will be reversed in the bottom walls for all cases. The minimum value of the Nusselt number in the three walls: hot wall, moving wall and bottom wall for all cases occurs at $Ri = 10$. This is related to the dominant buoyancy force in the mechanism of heat transfer.

4 Friction factor

Figure 6 represents the variation of skin friction with Richardson number for three cases studied in the present work, and for three walls for each case: moving wall, bottom wall and hot circular wall. The higher values of skin friction on the lid wall at $Ri = 0.01$ (dominant forced convection) compared with other values on the other walls and for other cases make these values seem to be closer to each other in the lower portion of the figure.

So, Table 6 shows the average skin friction values for the above cases. It is seen that the friction coefficients for $Ri = 0.01$ are much higher than that

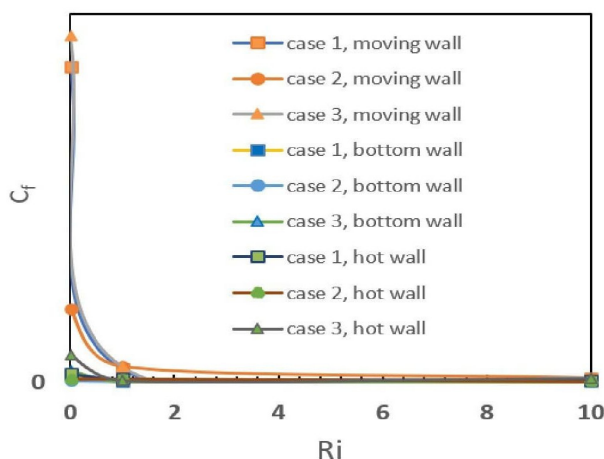


Figure 6: Average skin friction coefficient *versus* Richardson number on the moving, hot, and bottom walls.

at $Ri = 1.0$ and 10.0 , especially on the moving wall because the dominating forced convection produces an increased pressure drop on the moving wall, bottom wall and hot cylinder wall. Moreover, the values of friction coefficient on the lid wall are higher than that on the bottom wall due to the high velocity of fluid motion on the moving wall, whereas these values are higher on the hot cylinder wall with respect to the bottom cold wall because of high mixed convection in this region.

Table 6: Average skin friction on the moving, hot, and bottom walls.

Wall type	Ri	Case 1	Case 2	Case 3
Moving wall	0.01	$1.371 \cdot 10^{-3}$	$3.1536 \cdot 10^{-4}$	$1.5087 \cdot 10^{-3}$
Moving wall	1.00	$5.53 \cdot 10^{-5}$	$6.6222 \cdot 10^{-5}$	$6.5097 \cdot 10^{-5}$
Moving wall	10.00	$1.56 \cdot 10^{-5}$	$1.554 \cdot 10^{-5}$	$1.51829 \cdot 10^{-5}$
Bottom wall	0.01	$3 \cdot 10^{-5}$	$5.7376 \cdot 10^{-6}$	$4.9819 \cdot 10^{-5}$
Bottom wall	1.00	$2.29 \cdot 10^{-6}$	$2.6087 \cdot 10^{-6}$	$5.5419 \cdot 10^{-7}$
Bottom wall	10.00	$6.23 \cdot 10^{-7}$	$1.826 \cdot 10^{-7}$	$1.1374 \cdot 10^{-7}$
Hot wall	0.01	$3.4 \cdot 10^{-5}$	$1.0121 \cdot 10^{-5}$	$1.185 \cdot 10^{-4}$
Hot wall	1.00	$1.3 \cdot 10^{-5}$	$1.1176 \cdot 10^{-5}$	$4.7116 \cdot 10^{-6}$
Hot wall	10.00	$5.33 \cdot 10^{-5}$	$3.0551 \cdot 10^{-7}$	$1.53388 \cdot 10^{-5}$

Figure 7 shows the behaviour of pressure drop on the moving wall at different values of Richardson numbers. The behaviour is the same as that in the average friction factor.

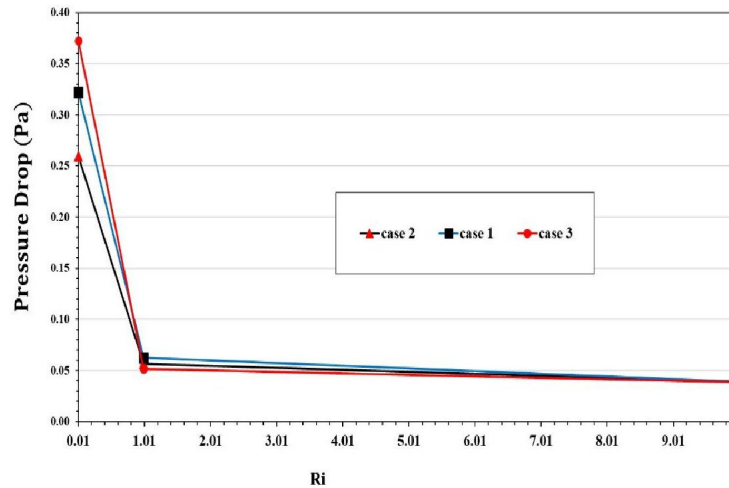


Figure 7: Pressure drop *versus* Richardson number on the moving wall.

5 Conclusions

The objective of the present study is to investigate the influences of the position of the hot circular cylinder on the behaviour of streamlines, isotherms, average Nusselt number and friction factor in a lid-driven trapezoidal cavity filled with water. The top wall moves as lid-driven with a constant speed. Three values of Richardson number ($Ri = 0.01$, 1.0 , and 10) are considered. It is concluded that:

1. At a low Richardson number ($Ri = 0.01$), the shear effects resulting from the motion of the top lid are predominant.
2. The higher velocity of fluid close to the lid-driven wall produces a significant distortion in the thermal plume.
3. When the natural convection is dominated ($Ri = 10$), the maximum stream function in case 1 (concentric cylinder) is higher than in case 3 (upper position of the inner cylinder) and case 2 (lower position of the inner cylinder), consequently.

4. The values of the mean Nusselt number in the moving wall are higher than that in the hot and bottom walls.
5. The maximum value of the Nusselt number in the moving and hot walls for both cases: case 1 and case 2 occurs at $Ri = 1$ (mixed convection).
6. The skin friction factors (frictional losses) for $Ri = 0.01$ are much higher than those at $Ri = 1$ and 10, especially on the moving wall.
7. The values of friction coefficient on the lid wall are higher than those on the hot and bottom walls.

Received 10 February 2023

References

- [1] Rosdzimin A.R.M., Zuhairi S.M., Azwadi C.S.N.: *Simulation of mixed convective heat transfer using lattice Boltzmann method*. Int. J. Automot. Mech. Eng. (IJAME) **2**(2010), 130–143.
- [2] Nemati H., Farhadi M., Sedighi K., Fattahi E., Darzi A.A.R.: *Lattice Boltzmann simulation of nanofluid in lid-driven cavity*. Int. Commun. Heat Mass **37**(2010), 10, 1528–1534.
- [3] Sheikhzadeh G.A., Qomi M.E., Hajjaligol N., Fattahi A.: *Numerical study of mixed convection flows in a lid-driven enclosure filled with nanofluid using variable properties*. Results Phys. **2**(2012), 5–13.
- [4] Chattopadhyay A., Sensarma S., Pandit S.K.: *Numerical simulations of mixed convection in a porous double lid driven cavity*. In: Proc. Int. Conf. on Mathematical Modeling And Computer Simulation with Applications, IIT Kanpur, Dec. 31, 2013 – Jan. 2, 2014.
- [5] Ögüt E.B., Kahveci K.: *Mixed convection heat transfer of ethylene glycol and water mixture based Al_2O_3 nanofluids: Effect of thermal conductivity models*. J. Mol. Liq. **224**(2016), 338–345.
- [6] Mastiani M., Kim M.M., Nematollah A.: *Density maximum effects on mixed convection in a square lid-driven enclosure filled with Cu-water nanofluids*. Adv. Powder Technol. **28**(2017), 1, 197–214.
- [7] Jahirul Haque Munshi M., Nusrat J., Golam M.: *Mixed convection heat transfer of nanofluid in a lid-driven porous medium square enclosure with pairs of heat source-sinks*. Am. J. Eng. Res. (AJER) **8**(2019), 6, 59–70.
- [8] Çakmak N.K., Durmazucar H.H., Yapici K.: *A numerical study of mixed convection heat transfer in a lid-driven cavity using Al_2O_3 -water nanofluid*. Int. J. Chem. Technol. **4**(2020), 1, 22–37.

- [9] Bhattacharya M., Basak Tanmay, Oztop H.F., Varol Y.: *Mixed convection and role of multiple solutions in lid-driven trapezoidal enclosures*. Int. J. Heat Mass Tran. **63**(2013), 366–388.
- [10] Mehmood Z., Javed T., Pop J.: *MHD-Mixed convection flow in a lid driven trapezoidal cavity under uniformly/ non-uniformly heated bottom wall*. Int. J. Numer. Method Heat Fluid Fl. **27**(2016), 6, 1231–1248.
- [11] Borhan Uddin M., Rahman M.M., Khan M.A.H., Saidur R., Ibrahim T.A.: *Hydro-magnetic double-diffusive mixed convection in trapezoidal enclosure due to uniform and nonuniform heating at the bottom side: Effect of Lewis number*. Alexandria Eng. J. **55**(2016), 2, 1165–1176.
- [12] Raizah Z.A., Ahmed S.E., Hussein A.K., Mansour M.A.: *MHD mixed convection in trapezoidal enclosures filled with micropolar nanofluids*. Nanosci. Technol.-Int. J. **9**(2018), 4, 343–372.
- [13] Mondal P., Mahapatra T.R.: *Minimization of entropy generation due to MHD double diffusive mixed convection in a lid driven trapezoidal cavity with various aspect ratios*. Nonlinear Anal.-Model. Contr. **25**(2020), 4, 545–563.
- [14] Sharif M.A.R.: *Laminar mixed convection in shallow inclined driven cavities with hot moving lid on top and cooled from bottom*. Appl. Therm. Eng. **27**(2007), 1036–1042.
- [15] Oztop H.F., Sun C., Yu B.: *Conjugate-mixed convection heat transfer in a lid-driven enclosure with thick bottom wall*. Int. Commun. Heat Mass Tran. **35**(2008), 779–785.
- [16] Salahi H., Sharif M.A.R., Rasouli S.: *Laminar mixed convective heat transfer in a shallow inclined lid-driven cavity filled with nanofluid*. J. Therm. Sci. Eng. Appl. **7**(2015), 4, 041016.
- [17] Kefayati G.H.R., Tang H.: *MHD mixed convection of viscoplastic fluids in different aspect ratios of a lid-driven cavity using LBM*. Int. J. Heat Mass Tran. **124**(2018), 344–367.
- [18] Ardalan M.V., Alizadeh R., Fattahi A., Rasi N.A., Doranehgard M.H., Karimi N.: *Analysis of unsteady mixed convection of Cu-water nanofluid in an oscillatory, lid-driven enclosure using lattice Boltzmann method*. J. Therm. Anal. Calorim. **145**(2021), 2045–2061.
- [19] Chen C.-L., Cheng C.-H.: *Experimental and numerical study of mixed convection and flow pattern in a lid-driven arc-shape cavity*. Heat Mass Transfer **41**(2004), 1, 58–66.
- [20] Parvin S., Nasrin R.: *Magnetohydrodynamic mixed convection heat transfer in a lid-driven cavity with sinusoidal wavy bottom surface*. J. Tri. Math. Soc. **12**(2010), 1–9.
- [21] Saha L.K., Monotos Chandra Somadder, Salah Uddin K.M.: *Mixed convection heat transfer in a lid driven cavity with wavy bottom surface*. Am. J. Appl. Math. **1**(2013), 5, 92–101.
- [22] Nasrin R., Alim M.A., Chamkha A.J.: *Modeling of mixed convective heat transfer utilizing nanofluid in a double lid-driven chamber with internal heat generation*. Int. J. Numer. Method Heat Fluid Fl. **24**(2014), 1, 36–57.
- [23] Mojumder S., Saha S., Rahman M.R., Rahman M.M., Khan Md. Rabbi, Ibrahim T.A.: *Numerical study on mixed convection heat transfer in a porous L-shaped cavity*. Eng. Sci. Technol.-Int. J. **20**(2017), 1, 272– 282.

-
- [24] Guo Z., Wang J., Mozumder A.K., Das P.K.: *Mixed convection of nanofluids in a lid-driven rough cavity*. AIP Conf. Proc. **1851**(2017), 020004.
- [25] Alesbe I., Ibrahim S.H., Sattar A.: *Mixed convection heat transfer in multi-Lid- driven trapezoidal annulus filled with hybrid nanofluid*. J. Phys.: Conf. Ser. **1973**(2021), 012065.